Effect of RRA Treatment on the Microstructure and Fatigue Behavior of 7020 Aluminum Alloy

Yong Wang, Yunlai Deng, Shengdan Liu, Zhaojun Shan, Jianguo Tang and Xinming Zhang

Abstract The fatigue crack growth (FCG) behavior and fatigue strength of 7020 aluminum alloy in an over aged treatment and two retrogression and re-aging (RRA) treatments were investigated. The microstructures and fractographies were observed by transmission electron microscopy (TEM) and scanning electron microscopy (SEM). The result showed that RRA-treated alloys have faster FCG rate than over aged alloy at lower ΔK region due to the dense non-shearable precipitates. And the RRA120 alloy re-aged at 120 °C/24 h has a relatively faster FCG rate than RRA150 alloy re-aged at 150 °C/12 h. RRA-treated alloys have higher fatigue strength than over aged alloy. The fatigue strength corresponding to 10^7 cycles of over aged, RRA120 and RRA150 conditions are 114, 129 and 118 MPa, respectively. The effect of RRA treatment on the fatigue property is mainly caused by its finer and more dispersed precipitates and narrower precipitate free zone (PFZ).

Keywords 7020 aluminum alloy · Retrogression and re-aging (RRA) treatment Microstructure · Fatigue crack growth · Fatigue strength

Y. Wang · Y. Deng · J. Tang (✉) · X. Zhang
Light Alloy Research Institute, Central South University, Changsha 410083, China
e-mail: jgtang@csu.edu.cn

Y. Wang · Y. Deng · S. Liu · Z. Shan · J. Tang · X. Zhang
Key Laboratory of Nonferrous Metal Materials Science and Engineering,
Ministry of Education, Central South University, Changsha 410083, China

Y. Deng · S. Liu · Z. Shan · J. Tang · X. Zhang
School of Materials Science and Engineering, Central South University,
Changsha 410083, China

Introduction

7020 aluminum alloy is widely used in high speed train because of its high specific strength, good formability and weldability [1]. One of the major problems during their use is the low resistance to stress corrosion cracking (SCC) in T6 temper. The resistance to SCC of the material can be significantly increased by two-stage over-ageing treatment T7X but it also reduces the strength. A new three-step heat treatment, commonly called retrogression and re-aging (RRA) treatment, solved the contradiction by enhance the SCC resistance of the alloy while retaining its original strength [2]. RRA treatment comprises three steps [3, 4]: (1) pre-aging heat treatment: the alloy is treated to the state of under aging or peak aging. (2) retrogression heat treatment: the alloy is treated at a high temperature for a short period of time so that part of precipitates formed during pre-aging are redissolved. (3) re-ageing heat treatment: the alloy is treated for a longer period of time at a lower temperature.

Many studies have shown that different aging treatments and the resultant microstructures have noticeable impact on the fatigue properties of precipitation hardening aluminum alloys [5, 6]. The microstructure characteristics such as grain size, primary phase morphology and recrystallization degree, which have significant influence on the fatigue property, do not change during ageing treatment. Therefore, the difference of fatigue properties in different ageing conditions is mainly caused by the difference of precipitates size and morphology in grain interior and grain boundary, and the precipitate free zone (PFZ) in grain boundary. Many researchers [7–9] have proposed that under aged alloys have better FCG resistance than peak aged and over aged alloys due to the reversibility of dislocation motion. But Gurbuz [10] found non-shearable coarse particles in over aged alloy retard FCG because the dislocations loop and bypass the precipitates and thus increase the strain hardening rate. Xia [11] proposed that the prolonged retrogression treatment and re-aging treatment of 7050 aluminum alloy was beneficial to FCG resistance because dislocations can slip freely in the spacing between the large precipitates. Therefore, it is necessary to do further research on the effect of ageing, especially RRA conditions, on the FCG and fatigue crack initiation, with a view to improving the fatigue behavior by heat treatment.

In the present work, an over aged condition and two RRA treatments with different re-ageing temperature and time were chosen to study the effect of aging treatment on the microstructure of the alloy. And the mechanism of the difference in fatigue crack initiation and FCG was further discussed.

Experimental

A commercial 7020 aluminum alloy has been used in this work. The chemical composition of the 7020 aluminum alloy are shown in Table 1. 7020 alloy was casted, homogenized, hot extruded, press quenched before aging treatment. Table 2 shows the details process of the over aged and two different RRA treatments.

The fatigue crack growth tests were conducted on a material testing system (MTS Landmark Servohydraulic Test System) according to ASTM Standard E647. Compact tension (CT) specimens were used and they were prepared by wire cutting from the extrusions in L-T orientation. The tests were conducted in constant load control mode at room temperature in laboratory air. The stress ratio ($R = \sigma_{min}/\sigma_{max}$) is 0.1 and the frequency of loading was 10 Hz.

TEM examinations were performed on the Tecnai G^2 20 ST microscope operated at 200 kV. The thin foils for TEM test were reduced to less than 100 μm by mechanical thinning and punched into discs with a diameter of 3 mm. The discs were thinned by twin-jet electropolishing subsequently at −30 °C and a potential difference of 20 V. The solution composition is 30% nitric acid and 70% methanol. The observation of fatigue fracture surface was finally inspected by SEM operating at 20 kV.

Results

Mechanical Properties Table 3 represents the hardness and tensile properties of the alloy. The tensile strength of RRA treated alloys is comparable to T6 temper. And the hardness and strength of RRA120 alloy are relatively higher than that of the RRA150 alloy. For the over aged alloy, the tensile strength decreased by 13.9% and yield strength decreased by 18.8% compared to RRA120 alloy. The elongation of the over aged, RRA120 and RRA150 alloys are 15.5, 14.9 and 15.1%, respectively.

Table 1 Chemical composition of 7020 alloy (wt%)

Zn	Mg	Mn	Cr	Zr	Ti	Cu	Fe	Si	Al
4.45	1.18	0.31	0.21	0.13	0.05	0.12	0.13	0.05	Bal.

Table 2 Heat treatment procedures for the alloy

Condition	Artificial aging treatment
Over aged	90 °C/12 h+170 °C/15 h
RRA120	90 °C/24 h+185 °C/ 105 min+120 °C/24 h
RRA150	90 °C/24 h+185 °C/105 min+150 °C/12 h

Table 3 Hardness and tensile properties under different aging conditions

Temper	Hardness (HV)	$\sigma_{0.2}$ (MPa)	σ_b (MPa)	δ (%)
Over aged	106.0	267.8	335.4	15.5
RRA120	121.9	330.0	389.5	14.9
RRA150	112.2	319.7	377.4	15.1

Microstructure Figure 1 represents TEM micrographs and SAED patterns of over aged and two RRA treated alloys. The grain interior precipitates in RRA120 and RRA150 alloys are obviously fine and dispersed. And obvious diffraction spots at 1/3 and 2/3 $\{220\}_{Al}$ in $<110>_{Al}$ projection can be observed in Fig. 1c, e. It is indicated that η' precipitates are major precipitates in RRA-treated alloys. On the contrary, the grain interior precipitates in over aged alloy are much coarser in Fig. 1a, and there are obvious additional spots close to 1/3 or 2/3 $\{220\}_{Al}$, indicating that a considerable number of η precipitates are formed during overageing treatment. The average diameter of precipitates which are estimated on several representative TEM images in over aged, RRA120 and RRA150 alloys are 10.8, 7.1 and 7.7 nm, respectively. It is apparent that the PFZ is much wider in over aged alloy than that in RRA-treated alloys. And the size of grain boundary precipitates in over aged alloy is much greater. Grain boundary precipitates in RRA150 alloy show slightly larger than RRA120 alloy due to its higher re-ageing temperature and it also bring about a wider PFZ (about 80 nm) than RRA120 alloy (about 64 nm), but both are narrower than over aged alloy (about 104 nm).

Fatigue Strength The S-N curves obtained in different aging conditions are showed in Fig. 2. The Stromeyer relationship [12], useful when there is no high stress downward concavity is:

$$\log_{10}(N) = A + B \log_{10}(S - E) \tag{1}$$

where: S is the stress or strain; N is the fatigue life; A, B are curve fit parameters; E is stress at very long life and must be less than all the stress or strain values in the data.

The fatigue life data of the three different aging conditions were fitted according to the above formula respectively, and the following fitting formula was obtained:

$$\text{Over aged: } \log_{10}(N) = 9.56 - 2.48 \log_{10}(S - 102.93) \tag{2}$$

$$\text{RRA120: } \log_{10}(N) = 9.24 - 2.25 \log_{10}(S - 118.90) \tag{3}$$

$$\text{RRA150: } \log_{10}(N) = 9.86 - 2.49 \log_{10}(S - 104.29) \tag{4}$$

We can found that the fatigue life of the alloy rises fast with the decline of the cyclic stress. When the cyclic stress level drops to a certain extent, the S-N curve gradually becomes horizontal. The fatigue strength corresponding to 10^7 cycles of over aged, RRA120 and RRA150 conditions are 114, 129 and 118 MPa,
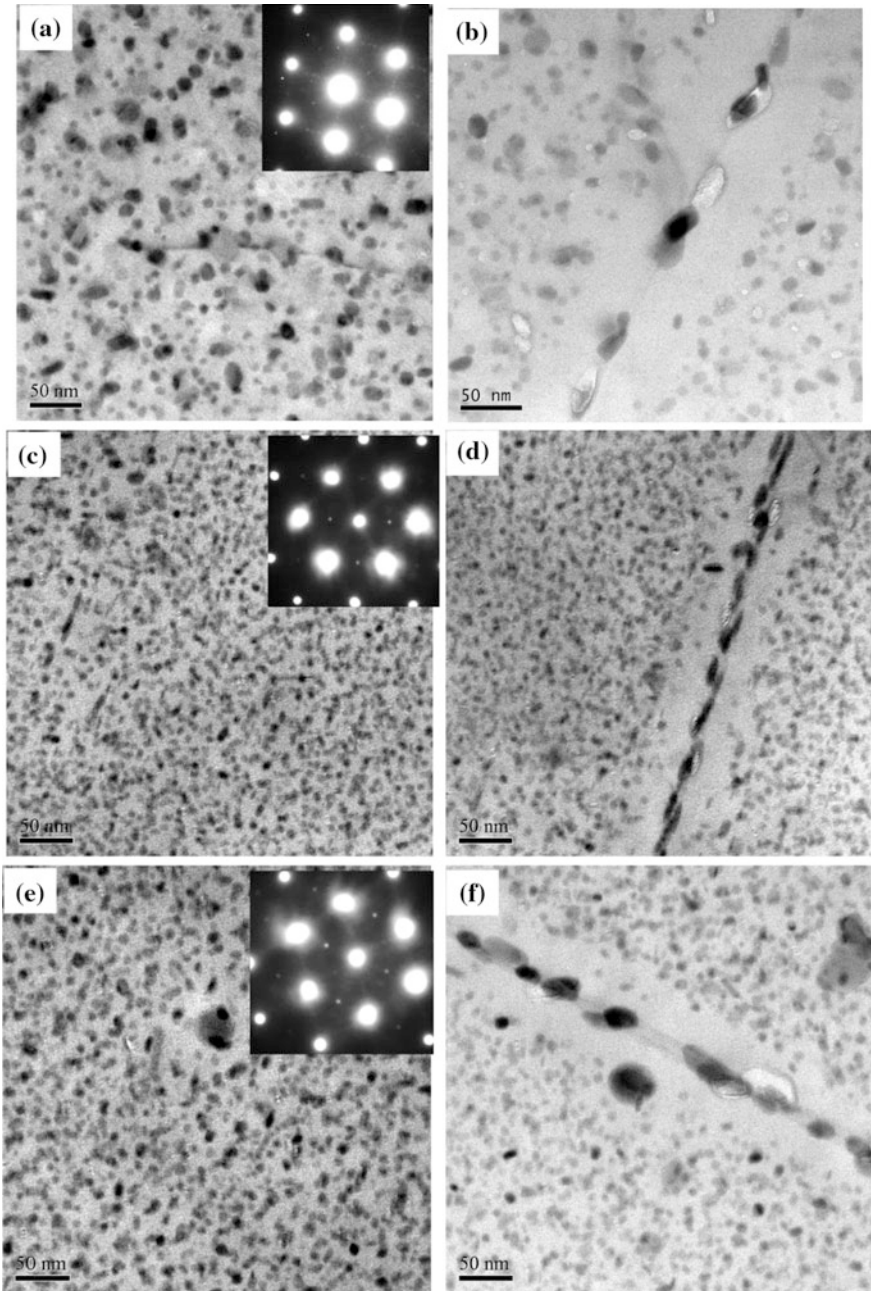
Fig. 1 TEM micrographs in different ageing treatments, **a**, **b** over aged, **c**, **d** RRA120, **e**, **f** RRA150

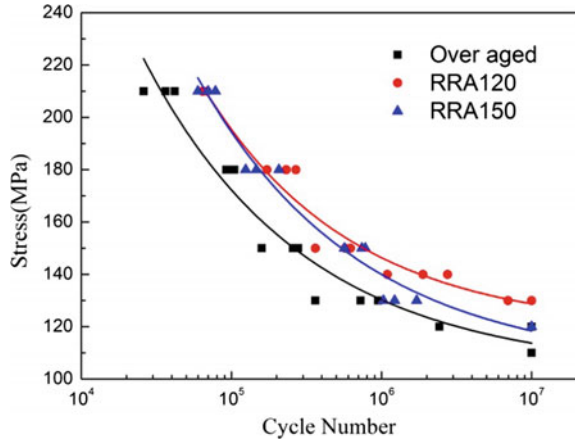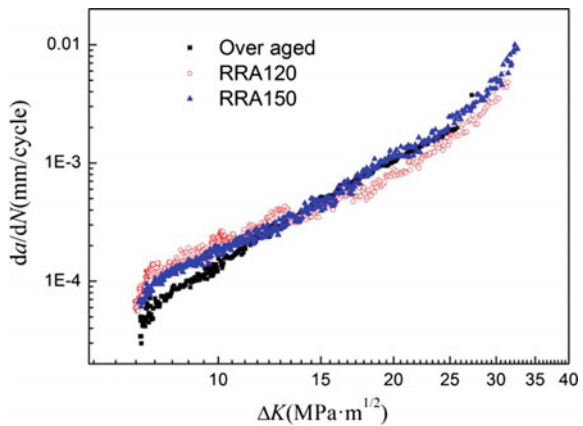**Fig. 2** S-N curves in
different ageing conditions

Fig. 3 FCG rate curves in
different ageing treatments

respectively. It is obvious that RRA treatments improve the fatigue strength of the
alloy compared to overaging treatment. And the fatigue strength of the alloy re-aged
at 120 °C for 24 h is higher than that re-aged at 150 °C for 12 h.

Fatigue Crack Growth The fatigue crack growth rate curves produced in different
aging conditions of the alloy are showed in Fig. 3. The linear part in the FCG curve,
which is called Paris region, complies with the following relationship:

$$\frac{da}{dN} = c(\Delta K)^n \tag{5}$$

where: c, n are material constants.

Table 3 lists the Paris constants (c and n) values obtained by fitting the above
formula and the values of da/dN at four specific ΔK levels. The c and n values for

the over aged alloy are 1.89×10^{-7} and 2.89. For the RRA120 alloy the values are 1.05×10^{-6} and 2.25, and for the RRA150 alloy they are 2.66×10^{-7} and 2.78, respectively. The c value affects the FCG rate in low ΔK region. It is the smallest in the over aged alloy and that of the RRA120 alloy is the largest. For instance, at $\Delta K = 8$ MPa $m^{1/2}$, the FCG rate of over aged alloy is 7.69×10^{-5} mm/cycle, lower than the RRA120 alloy with a FCG rate of 1.13×10^{-4} mm/cycle and the RRA150 alloy with a FCG rate of 8.26×10^{-5} mm/cycle. With the increase of ΔK value, the difference of FCG rate among different aging conditions is gradually reduced. The FCG rate of RRA120 condition becomes the smallest when the ΔK value exceeds 15 MPa $m^{1/2}$.

Fractography The fractographs in different ageing conditions are shown in Figs. 4, 5 and 6. At different aging conditions and FCG rates, facet, striations, secondary cracks, tear ridges and other typical features can be seen in fatigue fracture surface.

Figure 4 shows fracture surface in initiation regime of smooth specimen. Fatigue crack growth is always transgranular. It is noticed that small facets are observed in RRA120 alloy, while more large facets appear in RRA150 and over aged alloy. Gupta [13] proposed that the facet size in different aging conditions is determined by the accumulation degree of plastic strain.

Figure 5 shows fractographs in FCG Paris regime ($\Delta K = 15$ MPa $m^{1/2}$). Fatigue striations, which are characteristics of Paris regime, were used to calculate the local FCG rate by measured the spacing between them. Apparent striations can be seen in all aging conditions and the width of striations measured is in accordance with the calculated data in Table 3. The fatigue patchs and secondary cracks can also be observed.

Figure 6 shows fractographs in fatigue rupture region. Ductile fracture surfaces similar to the tensile fracture are characterized by a lot of dimples with broken second phases. The dimples in over aged and RRA150 alloy are relatively large and deep due to their good plasticity.
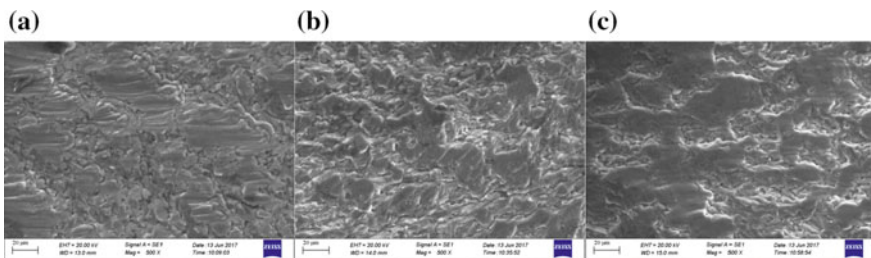

Fig. 4 SEM fractographs in initiation region in different ageing conditions, **a** Over aged, **b** RRA120, **c** RRA150
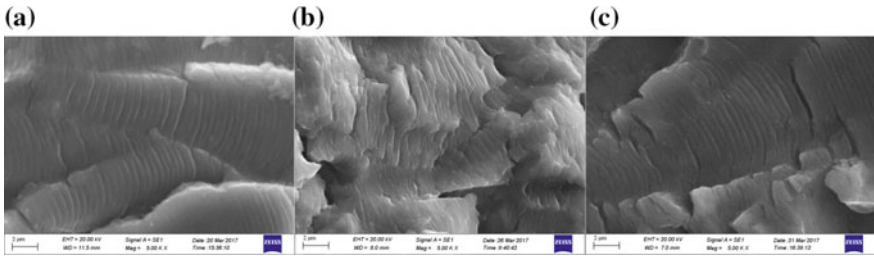
Fig. 5 SEM fractographs in Paris region in different ageing conditions, **a** over aged, **b** RRA120, **c** RRA150
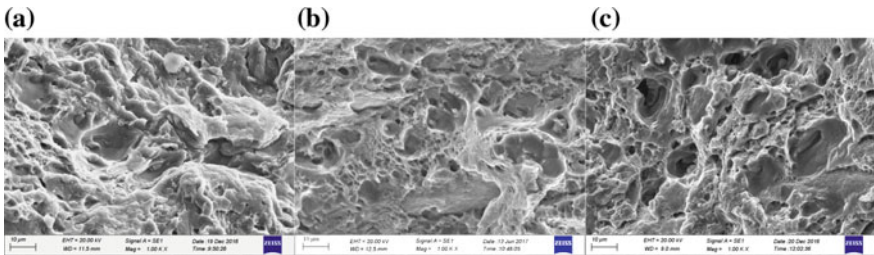

Fig. 6 SEM fractographs in rupture region in different ageing conditions, **a** over aged, **b** RRA120, **c** RRA150

Discussion

The total fatigue life of materials is composed of two parts: the cycle number of fatigue crack initiation and the cycle number of fatigue crack growth to fracture. And the FCG stage contains near-threshold region, Paris region and final rupture region. The fatigue crack initiation and FCG at lower ΔK region are mainly discussed.

A large number of studies [14] have shown that the alloys in under aged condition have good FCG resistance due to the their small precipitates and the reversibility of dislocations movement in the plastic zone at the tip of fatigue crack. Since the small precipitates in under aged alloys are coherent and shearable, dislocations move back to the opposite direction on the slip plane when the stress is unloaded. It reduces the local stress concentration and the plastic accumulation, thus reducing the FCG rate. On the other hand, non-shearable precipitates retard the reversible slip of dislocation. The change in the size of the precipitates causes different mechanisms when the dislocation passes through the particles. Kovács [15] have studied both the cutting and bypassing mechanisms and got the following equations:

$$\tau_{cutting} = 1.44(\frac{\Gamma}{Gb})^{3/2}(\frac{fR}{b})^{1/2}G \tag{6}$$

$$\tau_{orowan} = 0.85\sqrt{\frac{f}{2}} \cdot \frac{G}{2\pi\sqrt{1-v}} \cdot \frac{bln(1.57R/r_0)}{R\left(1 - 1.57\sqrt{f/2}\right)} \tag{7}$$

where: $\tau_{cutting}$ and τ_{orowan} are the critical shear stress of the cutting and bypassing mechanisms, R is the average particle radius, f is the volume fraction of precipitates. It can be seen from the above equation that the critical shear stress of the cutting mechanism enhanced with the increase of the volume fraction and the average particle radius, while the bypass mechanism decreases with the decline of volume fraction and the increase of average particle radius. There is a critical size, the dislocations cut off the precipitates when their size is less than it, and bypass the precipitates when their size is greater than it. The critical size is about 3 nm for Al–Zn–Mg alloy [15–17]. Therefore, the precipitates in RRA conditions are not sheared although they are relatively small.

At lower ΔK region, the plastic zone at the front of fatigue crack is very small. This means the slip distance of dislocations is short while the spacing of precipitates in the over aged alloy is relatively large. The probability of dislocations interacting with precipitates is low in over aged alloy which has large precipitates size and wider spacing, thereby promoting the slip reversibility, finally reducing the FCG rate. So the FCG rate of over aged alloy is relatively slower. The RRA alloys show high FCG rate because the dense precipitates retard the reversible slip of dislocations, and RRA120 alloy has a relatively faster FCG rate than RRA150 alloy at lower ΔK region. Xia [11] also found that larger precipitates caused by prolonged re-aging time can reduce the FCG rate in Al–Zn–Mg–Cu alloy. At higher ΔK region, the plastic zone is large and dislocation slip distance increases greatly. The precipitates both in over aged alloy and RRA treated alloys retard the reversible slip of dislocations seriously. But the wider PFZ and the larger grain boundary precipitates in over aged alloy make it easy to crack and promote a faster FCG.

In contrast to the FCG rate, the RRA120 alloy has the highest fatigue life and fatigue strength limit. Suresh [18] have pointed that the proportion of fatigue crack initiation can reach 80% of the total fatigue life in the smooth specimen. Therefore, the results of fatigue life are not inconsistent with the FCG results. The wide PFZs and coarse grain boundary precipitates are detrimental to fatigue behavior. The soft PFZs lacking solute atoms are prone to plasticity localization due to their lower strength. Furthermore, the large incoherent grain boundary precipitates are easily cracked from the interface with the matrix and promote the formation of voids in grain boundary, thus results in the initiation of fatigue crack [19]. From Fig. 1, it is obvious that the width of PFZ in RRA alloys are narrower than that in over aged alloy, especially the RRA120 alloy, which has a PFZ width of only 64 nm compared to the over aged alloy with a PFZ width of 104 nm. The size of grain boundary precipitates in over aged alloy is the largest and it is the least in RRA120 alloy. In addition, the dense precipitates which are non-shearable in nature in the

RRA alloy lead to more homogeneous deformation and the absence of localized plasticity, and reduce the possibility of void formation. Therefore, RRA treated alloys have relatively high fatigue life and fatigue strength limit.

Conclusions

(1) The precipitates in RRA-treated alloys are fine and dense compared to coarse precipitates in over aged alloys. And the size of precipitates in RRA120 is smaller than that of the RRA150 alloy. The width of PFZ in over aged alloy, RRA120 and RRA150 alloy are 104, 64 and 80 nm, respectively.
(2) RRA-treated alloys have faster FCG rate than over aged alloy at lower ΔK region due to the dense non-shearable precipitates. And RRA120 alloy has a relatively faster FCG rate than RRA150 alloy.
(3) RRA-treated alloys have higher fatigue strength than over aged alloy. The fatigue strength corresponding to 10^7 cycles of over aged, RRA120 and RRA150 conditions are 114, 129 and 118 MPa, respectively.

References

1. Xiao T, Deng Y, Ye L, et al. Effect of three-stage homogenization on mechanical properties and stress corrosion cracking of Al-Zn-Mg-Zr alloys[J]. Materials Science and Engineering: A, 675 (2016) 280–288.
2. Cina B. Reducing the susceptibility of alloys, particularly aluminum alloys to, to stress corrosion cracking: 1974.
3. Feng D, Zhang X M, Liu S D, et al. The effect of pre-ageing temperature and retrogression heating rate on the microstructure and properties of AA7055[J]. Materials Science & Engineering A, 588(5) (2013) 34–42.
4. Feng D, Zhang X M, Liu S D, et al. Non-isothermal "retrogression and re-ageing" treatment schedule for AA7055 thick plate[J]. Materials & Design, 60 (2014) 208–217.
5. Desmukh MN, Pandey R K, Mukhopadhyay A K. Effect of aging treatments on the kinetics of fatigue crack growth in 7010 aluminum alloy[J]. Materials Science & Engineering A, 435–436(5) (2006) 318-326.
6. Wang Y L, Pan Q L, Wei L L, et al. Materials & Design, 55 (2014) 857–863.
7. Hornbogen E, Gahr K H Z. Microstructure and fatigue crack growth in a γ-Fe-Ni-Al Alloy[J]. Acta Metallurgica, 24(6) (1976) 581–592.
8. Chen J Z, Zhen L, Yang S J, et al. Effects of precipitates on fatigue crack growth rate of AA 7055 aluminum alloy[J]. Transactions of Nonferrous Metals Society of China, 20(12) (2010) 2209–2214.

9. Xue X L, Zheng Z Q, Hu F, et al. Effect of aging conditions on the fatigue crack propagation rate of 2A97 aluminum-lithium alloy[J]. Rare Metal Materials and Engineering, 2016(12) 3319–3324.

10. Gurbuz R, Sarioglu F. Fatigue crack growth behaviour in aluminium alloy 7475 under different aging conditions[J]. Materials Science and Technology, 17(12) (2001) 1539–1543.

11. Xia P, Liu Z, Bai S, et al. Enhanced fatigue crack propagation resistance in a superhigh strength Al–Zn–Mg–Cu alloy by modifying RRA treatment[J]. Materials Characterization, 118 (2016) 438–445.

12. ISO. 12107:2012(E) Metallic materials — Fatigue testing — Statistical planning and analysis of data[S]. 2012.

13. Gupta V K, Agnew S R. Fatigue crack surface crystallography near crack initiating particle clusters in precipitation hardened legacy and modern Al–Zn–Mg–Cu alloys[J]. International Journal of Fatigue, 33(9) (2011) 1159–1174.

14. Zaiken E, Ritchie R O. On the development of crack closure and the threshold condition for short and long fatigue cracks in 7150 aluminum[J]. Metallurgical and Materials Transactions A, 16(8) (1985) 1467–1477.

15. Kovács I, Lendvai J, Ungar T, et al. Mechanical properties of AlZnMg alloys[J]. Acta Metallurgica, 28(12) (1980) 1621–1631.

16. Han N M. Investigation on the fracture toughness of 7050 aluminium alloy thick plate[D]. Central South University, 2011.

17. Marlaud T, Deschamps A, Bley F, et al. Evolution of precipitate microstructures during the retrogression and re-ageing heat treatment of an Al–Zn–Mg–Cu alloy[J]. Acta Materialia, 58 (14) (2010) 4814–4826.

18. Suresh S. Fatigue of Materials[M]. Cambridge University Press, 1999.

19. Chen X, Liu Z, Xia P, et al. Transition of crack propagation from a transgranular to an intergranular path in an overaged Al-Zn-Mg-Cu alloy during cyclic loading[J]. Metals & Materials International, 19(2) (2013) 197–203.